ISSN 1392-1207. MECHANIKA. Vol. 29, No. 2, 2023: 88–96

Investigation of Impact Performance of STF Impregnated Composites

Murat Berkay ZEKA*, Ayhan AYTAÇ**
**National Defence University, 34334 Yenilevent, Istanbul, Turkey, E-mail: mbzeka@kho.msu.edu.tr*
***National Defence University, 34334 Yenilevent, Istanbul, Turkey, E-mail: aytac@kho.msu.edu.tr*
https://doi.org/10.5755/j02.mech.31069

1. Introduction

Fibers such as aramid and ultra-high molecular weight polyethylene (UHMWPE) provide mobility to the user with their lightness, they have become preferred materials with their impact resistance and other mechanical properties at high strain rates. With the recent developments, it has been understood that these materials can be strengthened with different additives to improve their properties. Different chemicals and other additives can be used to improve the thermal, wear resistance, impact resistance of the composites.

One of the additives that have recently been used to improve impact resistance is the shear thickening fluid (STF). STF is a non-Newtonian fluid/colloidal dispersion that the viscosity of the liquid suddenly increases with rise of shear rate [1]. STF's are also known as dilatant liquid. After the shear stress exceeds a critical point, the STF shifts to solid phase. The opposite is a shear-thinning fluid, in which the viscosity decreases with an increase in the stress ratio. Many researchers have presented approaches that will explain the mechanism of shear thickening. Some of the most accepted theories in literature are the Order-Disorder Theory and Hydrocluster Theory [2-7]. STF is also used for other applications such as vibration damping [8-9].

There are several approaches to understand the general characteristics and behavior of STF's. A few factors affecting the rheological properties of suspensions were investigated. Some actors determining the rheological properties of STF are the volume fraction [10], interactions between the solid and the liquid phase and the shapes and sizes of the grains [11, 12]. There are also other factors such as temperature of the fluid and hardness of the particles [13, 14]. Another factor affecting the rheological behavior of STF is the particle distribution. Particle dispersion and shear rate affect the behavior of colloid suspensions. When the particle size distribution is large (from 0.1 mm to 1 cm), the interactions between the particles and the surrounding fluid can change. For relatively small strain rates, the thinnest particles are usually very sensitive to Brownian motion effects or colloidal forces, while coarse particles experience friction or collision contacts or hydrodynamic forces [15].

Studies on STF-impregnated composite fibers have recently become popular in the literature [16-20]. Majumdar et al. [21] tested STF-impregnated Kevlar fabrics using a drop test examined the damped energy by differantiating the sections: the elastic section, the slip/fracture section, and the deformation section.

Multiphase STF-impregnated composite fibers are becoming more popular in current studies [22]. Multiphase STFs are created by adding another phase such as nanotubes, metallic and ceramic particles. Gürgen and Kuşhan [23] fabricated multi-phase STF with silica, PEG 400, and silicon carbide particles with a size of 20 nm and as an additional additive. STF has a weight fraction of 15% silica, 60% PEG and 25% silicon carbide. Yarn pullout and drop tests were performed from different heights. In addition, microstructure studies and studies have been conducted to understand the elasticity of the fiber. It was understood that the shear thickening mechanism of single-phase STF is better than multi-phase liquid. However, multi-phase STF's energy damping is superior to single-phase STF.

This research paper presents the effect of weight fraction of silica in the STF on the ballistic performance of STF impregnated aramid fibers under low-speed impact and ballistic impact scenarios. Silica-polyethylene glycol based STF is produced. Silica ratios are determined as 30%, 40% and 50%. Although a lot of interest has been shown for the ballistic performance of the STF-Aramid fabrics, there are few research based on standards such as NIJ and evaluation of back face signature (BFS) values of fabrics.

2. Materials and methods

Kevlar 620 fabric is selected for STF impregnation. Kevlar is suitable for accommodating different additives. As shown in Figure 1 the fabrics were cut in sizes of 150 mm x 100 mm for the drop test and 400 mm × 400 mm for the ballistic test. Silica and polyethylene glycol were selected for fabrication of STF. Silica ratios were determined as 30%, 40% and 50%. AEROSIL 200 was selected as silica particles and PEG 400 as polyethylene glycol. Properties of AEROSIL and PEG 400 are presented at Tables 1 and 2.

Table 1

AEROSIL 200 properties

Density, g/cm^3	2,2
pH	3,7-4,7
Particle Size, nm	12
Surface Area, m^2/g	200±25

Table 2

PEG 400 properties

Density, g/cm^3	1.128
pH	5-7
Viscosity	90.0 cSt at Room Temp.
Vapor Pressure	<0.1 hPa (20 °C)

Due to its non-toxic structure and thermal stability, PEG 400 is a convenient agent. The weight fraction of silica in the STF was calculated using Eq. (1):

$$w\% = \frac{S}{F} \times 100, \quad (1)$$

where: *s* is the weight of silica; *F* is weight of STF. Due to its nature STF presents high viscosity under shear, so the mixing process should be carried out with other mixers such as sonic homogenisers. To ensure uniform distribution of silica particles in PEG, STF was mixed with ethanol. Ethanol also allows STF to be more easily absorbed by the Kevlar fabric. Silica and PEG 400 were mixed mechanically for 15 minutes. After that, ethanol was added to the suspension and mechanical mixing continued for another 10 minutes. Table 3 shows the mixing ratios of ratios of the prepared STF's. After the mechanical mixing was completed, the STF was sonicated with 50% pulse at a temperature of 50ºC using the VibraCell Sonics VCX 750 sonic homogenizer.

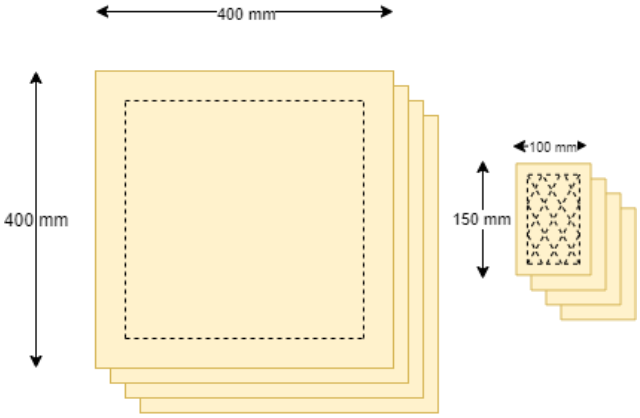

Fig. 1 Aramid fabrics and stitch pattern

The sonic mixing duration is 45 minutes, the time when silica agglomeration completely dispersed in the 30%. Silica is agglomerated on the top of the fluid, and it is observed until dispersion. However, with an increase in the silica ratio, the time is extended for the agglomeration in the mixture to dissipate. For this reason, different durations have been tried for other liquids and the most ideal times for which the agglomeration is distributed have been determined. Sonic homogenization is an effective method of providing a homogeneous distribution for such fluids with high viscosity.

Table 3

STF weight fractions and shear homogenization durations

Sample name	Silica ratio	PEG ratio	Ethanol ratio	Mixing time, minutes
% 30	% 30	%70	% 150	45
% 40	% 40	% 60	% 200	60
% 50	%	% 50	% 250	90

To ensure that the liquid is completely distributed over the fabrics a brush is used. Fabrics were impregnated for 15 minutes. It is compressed with a double roller so that excess liquid is removed from the fabric and the liquid spreads uniformly through the fabric. Then the fabrics were left in the oven for half an hour at a temperature of 80ºC to evaporate the ethanol. The Kevlar fibers are then stitched together for the ballistic and drop test.

2.1. Low-speed impact tests

Low-speed impact tests were performed using the Instron CEAST 9350 Drop Tower Impact System at the Materials Laboratory of the Mechanical Engineering Department of National Defence University depicted in Fig. 2. Test specimen is subjected to impact with a striker with a hemispherical tip. Since parameters such as the mass of the impact force and the height of the fall are known in advance, the potential energy of the drop weight is calculated before the test. A witness glass fiber plate with a thickness of 15 mm [0/90] was placed behind it to prevent Kevlar fabrics from slipping. Witness glass plate is also useful for observing the performance of fabrics more clearly.

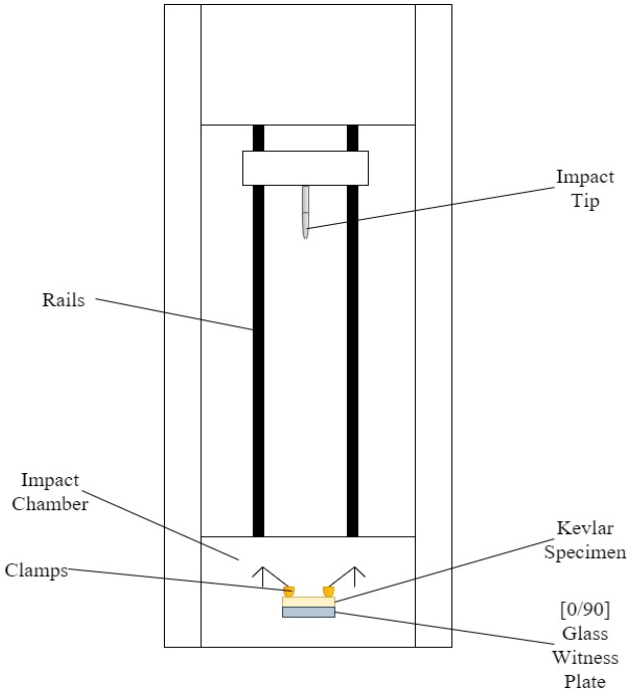

Fig. 2 Drop test instrument

As shown in Fig. 3, a pulse tip with an ogive geometry with a diameter of 16 mm and a length of 50 mm was used in weight reduction tests. The impact tip with a hardness of 60 Rockwell is made of DIN 1.2550 steel. The CRH value defined as the ratio of the radius of curvature of the impact tip *s* to the diameter *d* of the impact tip *s*/*d* is 1.

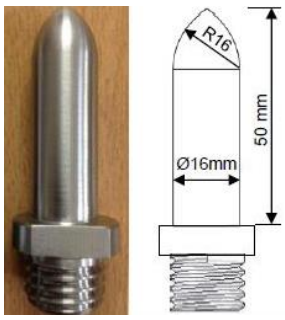

Fig. 3 Low speed impactor tip

2.2. Ballistic impact tests

According to NIJ 0101.06 [24], there are criterias such as ambient conditions and the angle of arrival of the bullet. The ambient temperature of the shot should be 21°C ± 2.9°C and the relative humidity should also be 50% ±

20%. In addition, there should be a distance 15 ± 1.0 meters between the barrel and the test sample. Chronographs for measuring bullet velocity should be 2.5 ± 0.025 m away from the support. As another requirement, the angle of arrival of the bullet must be less than 5º at the time of impact. Shots that hit the test sample when the bullet is fired at larger angles from this angle are not considered as "fair" hits.

There are several procedures that must be carried out for compliance with the test before the ballistic test. A support material made of Roma Plastilina clay is placed on the back of the armor sample, which is mentioned in the NIJ standards. As a result of this test, known as the P-BFS test, the cavity formed on the back of the armor is clearly visible along with the clay, so it becomes clear whether the armor provides the necessary protection.

Level II ballistic parameters are selected for shot test. Since the samples are not ballistic plates, Level II parameters are suitable for observing the BFS values. Level II body armor is an ideal level for law enforcement agencies. This kind of protection is usually found in soft body armored vests, it is usually the lightest, most flexible, and easiest to hide. The characteristics of the projectile are given in Table 4.

Table 4

Bullet parameters

NIJ Level	Projectile	Projectile speed	Weight
II	9 mm FMJ RN	398±9,1 m/s	8 gr

According to NIJ standards, 6 shots per sample are required. The first, second and third shots must meet the requirements of the edge-to-edge shooting distance, the minimum edge-to-edge shooting distance should not exceed 76 mm from the edge of the panel. The fourth, fifth and sixth shots can be located at any point on the sample but must be collected in a circle with a diameter of 100 mm. Considering these conditions, a shooting pattern was created.

3. Results and discussion

3.1. Rheologic behavior of STF

Rheological measurements and microstructure studies were carried out to understand the general behavior of STF's. For rheological measurements, TA Instruments Ares Rheometer with concentric cylinder with a length of 40 mm, an inner diameter of 32 mm and an outer diameter of 34 mm was used.

After the ethanol in the STF was evaporated, rheological measurements were conducted at room temperature. Fig. 4 shows the viscosity-shear rate curve of liquids. Liquids were able to show the thickening effect. However, no data could be retrieved from the 50% silica because the fluid is solidified after ethanol evaporation. Rheologic behavior of the fluids shows that there are two regions: shear-thinning and shear-thickening. The critical shear rate is the rate at which the liquid begins to thicken.

JEOL JCM 6000 PLUS Scanning Electron Microscope (SEM) device was used to study the microstructure of the liquid. Fig. 5 shows STF with 40% silica ratio. It is observed that STF solidifies and becomes gel-like in the high vacuum environment.

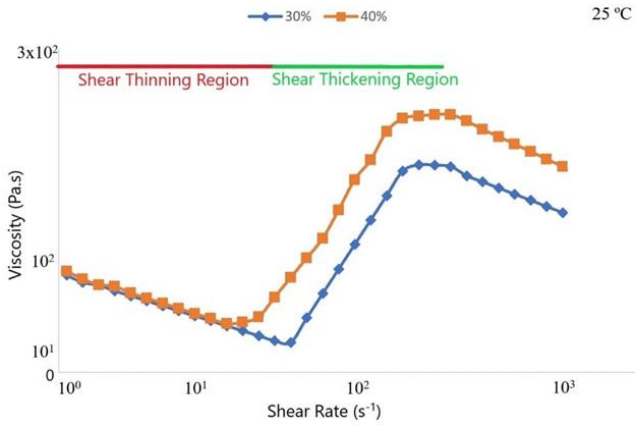

Fig. 4 Steady-shear rheology of STF's at ambient temperature

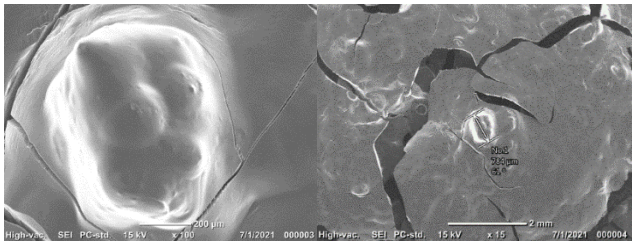

a b

Fig. 5 a) STF cluster; b) STF cluster

3.2. Characteristics of STF/Fabric

3.2.1. Drop test results

Low-velocity dynamic impact tests were carried out for both neat and STF impregnated fabric samples. Drop tests were performed with an energy of 300 J and it was examined how much energy the structure damped. As a result of low-speed impact tests, energy data from the force-displacement-time curves were created using the program. The specimen is fixed from 4 points on the sample with a horizontal clamp element consisting of a solid steel body. Thus, it is ensured that the force transmitted during the impact does not affect the results.

The damage on the fabrics and the witness plate has been examined. The depth and diameter of the puncture in the fabrics were measured, the damped energy and force-displacement graphs were created. Images of the samples and the witness plates are depicted in Fig. 6.

Sewing threads of the dry Kevlar specimen were mostly ripped, damage was observed on the fibers of the primary zone, which directly handled the damage, and the secondary zone, which contributed to the damping of the impact. Dry Kevlar specimen absorbed 140 J of energy, the penetration depth was recorded as 15.90 mm and the damage diameter was recorded as 25.40 mm. 30% STF/Kevlar samples showed detachments in the sewing threads. Damage in the primary zone is seen more clearly. % 30 STF/Kevlar specimen absorbed 221 J of energy, the penetration depth was recorded as 10.30 mm and the damage diameter was recorded as 18.31 mm. The structural integrity of the threads in the secondary zone preserved better and the damage remains only at the point of impact. The detachments observed on the sewing threads in 40% STF/Kevlar samples are very small. The highest energy absorbing was recorded as 232 J in the 40% STF/Kevlar.

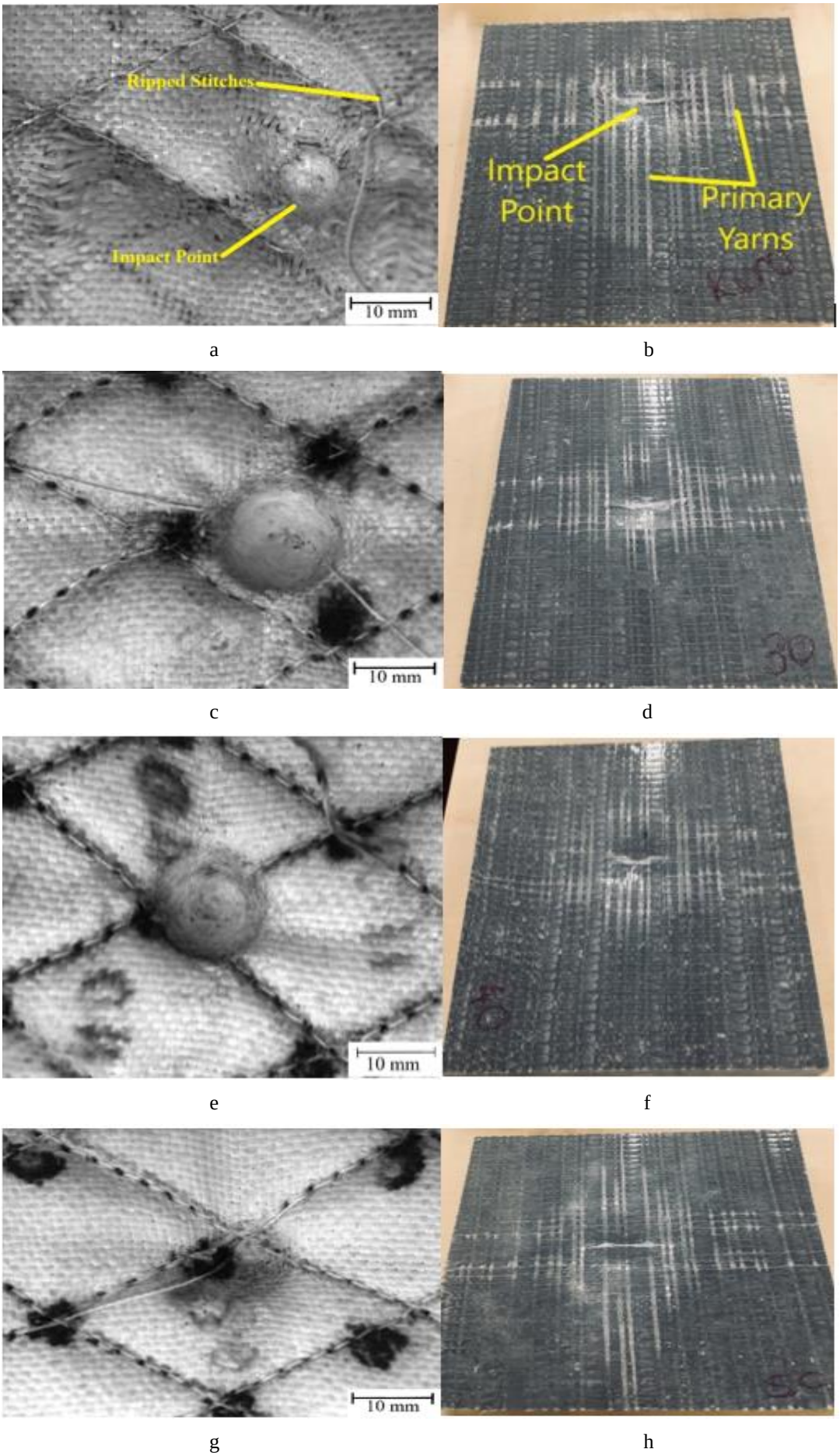

Fig. 6 a) Dry Kevlar; b) Dry Kevlar's witness plate; c) 30% STF/Kevlar; d) 30% STF/Kevlar's witness pate; e) 40% STF/Kevlar; f) 40% STF/Kevlar's witness plate; g) 50% STF/Kevlar; h) 50% STF/Kevlar's witness plate

sample. The penetration depth was recorded as 8.39 mm and the damage diameter was recorded as 14.80 mm. Just like with the 40% STF/Kevlar, 50% STF/Kevlar samples depicted few detachments on the sewing threads. However, the damped energy decreased, obtained as 227 J. The depth was recorded as 7.26 mm and the damage diameter as 11.93 mm.

The force-time, energy-time and force-displacement graphs obtained from the 300 J reduction tests are shown in Fig. 7. There is an increase in impact damping and the time spent by the striking mass on Kevlar fabrics was observed with an increase in the silica ratio, as well as an increase in the time spent on Kevlar fabrics. It has been noted that the "Hertzian threshold" at which the damage to the witness samples began is improved. At the Hertzian damage threshold point, the formation of matrix cracking or delamination in the glass composite occurs. Table 5 shows the results of the drop test. With an increase in the proportion of silica in liquids impregnated with Kevlar fabrics, size of the damage gets smaller. The size of the cracks on the upper side of the witness plate placed on the back was also measured and the damage was examined.

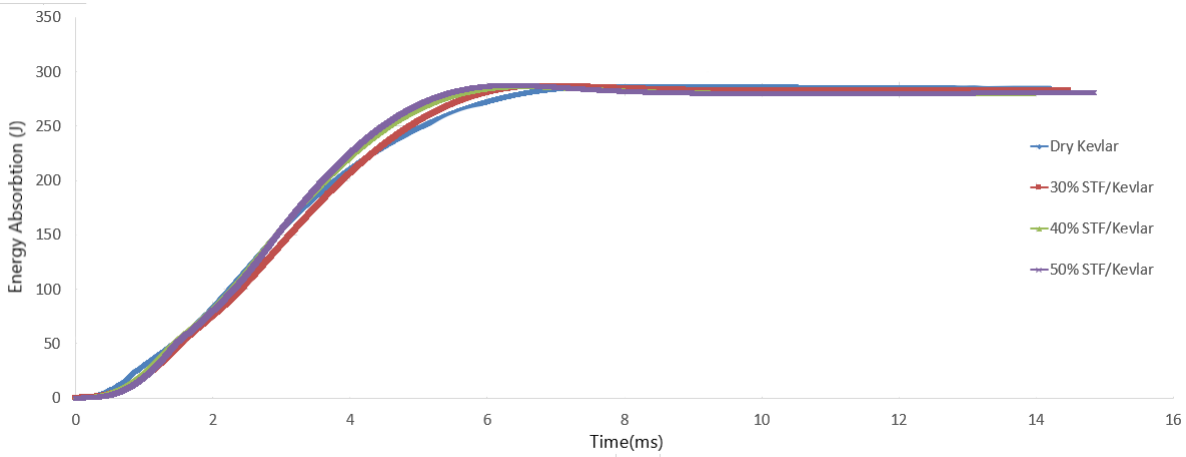

a

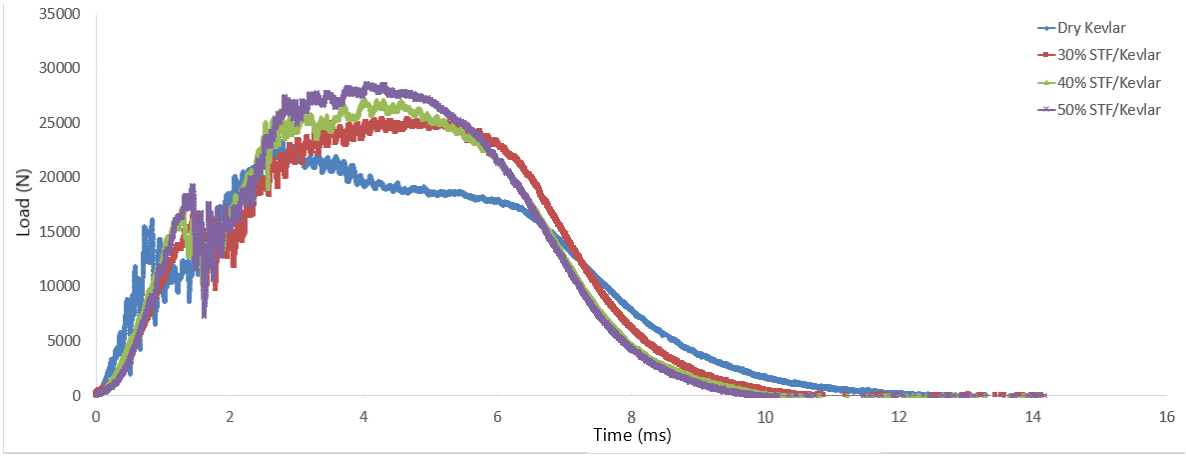

b

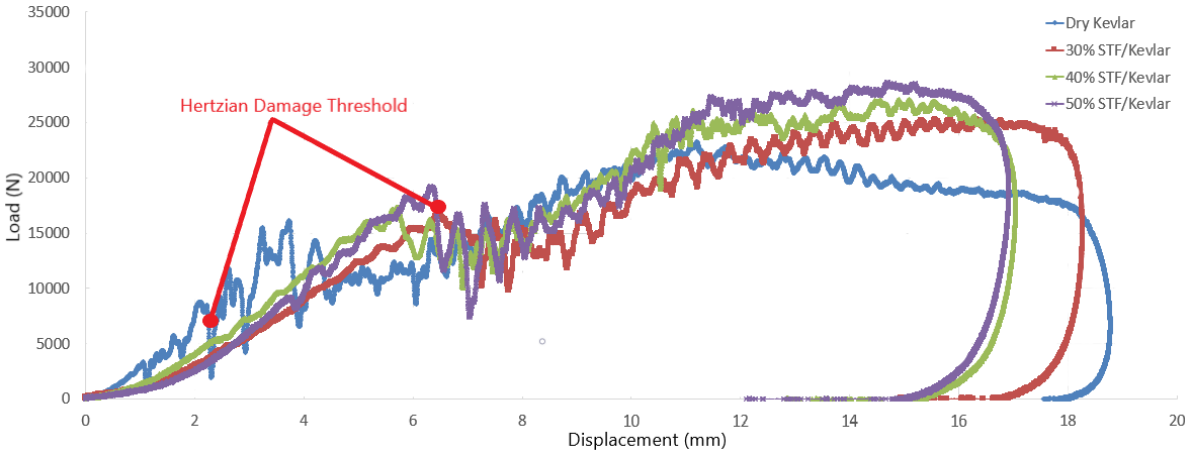

c

Fig. 7 a) Absorbed energy-time graph; b) Load-time graph; c) Load-displacement graph

Table 5

300J Drop test results

	Dry Kevlar	30% STF/Kevlar	40% STF/Kevlar	50% STF/Kevlar
Kevlar penetration depth, mm	15,90	10,30	8,39	7,26
Kevlar penetration diameter, mm	25,40	18,31	14,80	11,93
Witness plate penetration depth, mm	4,5	3,32	2,63	2,48
Absorbed energy, J	140	221	232	227
Maximum load, N	23238,98	25282,11	27061,18	28631,75
Time, ms	2,79	4,04	4,20	4,28
Impact speed, m/s	4,50	4,50	4,50	4,50

3.2.2. Ballistic test results

The experimental results were compared based on the BFS of the fabrics. The trauma values allow evaluating and comparing fabrics for ballistic efficiency. The effect of different ratios of STF on ballistic performance and compliance with NIJ Level II were discussed based on the collected results.

Images of fabrics after the ballistic tests are given in Fig. 8. All trauma values of dry Kevlar specimen were below the 44 mm specified as standard. Bullets stopped at 15th layer. The sample is partially penetrated, the inlet diameter of the bullet on the front side is relatively medium in size, fiber pullout has occurred at the last layer. Fiber damage have been observed on the front face, the fibers can be decoupled with a very small force. For 30% STF/Kevlar specimen, desired trauma values were obtained for first 4 shots. However, 5th and 6th the shots had a complete penetration. For 30% STF/Kevlar specimen, it is observed that the STF didn't distributed homogeneously to the fabrics and seperation has occured between the layers after couple of shots, which decreases ballistic performance.

All trauma values were below the 44 mm for 40% STF/Kevlar sample. Bullets stopped at 15th layer. The sample is partially penetrated, and it has been observed that the inlet diameters of the bullets are narrower than all the samples. Fiber pullout were observed at bullet penetration points. On the other hand, it was observed that 2 out of 6 shots did not leave any kind of damage on the back surface of the sample (Fig. 8, c) which also leads that 40% STF/Kevlar specimen is superior to other ones. The sample with the highest resistance in terms of damage was 40% STF/Kevlar by visual examination. Like 40% STF/Kevlar samples, improvement of damage absorbtion for 50% STF/Kevlar had recorded. Fiber pullout and breakage were observed at 5 shot locations at backface. Increase in ballistic performance was expected as the silica ratio increase.

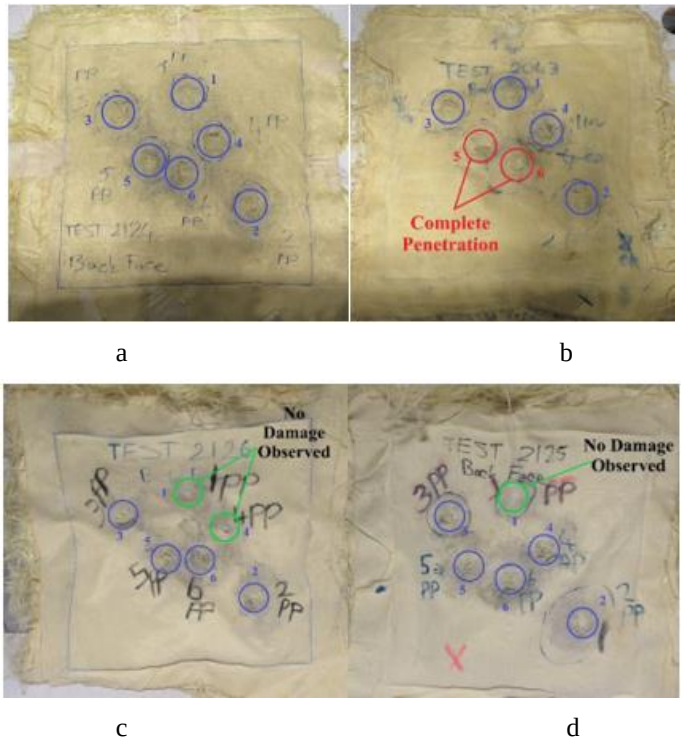

a b

c d

Fig. 8 a) Dry Kevlar samples; b) 30% STF/Kevlar; c) 40% STF/Kevlar; d) 50% STF/Kevlar

Although, trauma values were better than untreated dry sample, 50% STF did not give the best results. Table 6 shows the results of the ballistic test of samples against 9 mm threat. The comparison of the trauma values and averages in the shots is given in Fig. 9.

The difference between the highest and lowest trauma values in dry Kevlar samples was recorded as 8.02 mm. 30% STF/Kevlar sample performed 2% better than plain fabrics based on obtained trauma values. 50% STF/Kevlar fabrics showed 15% better ballistic performance than plain fabrics. 40% STF/Kevlar sample showed the best ballistic performance among them. It showed 26.17% superior ballistic performance compared to untreated Kevlar samples according to average BFS.

Table 6

Ballistic test results

	1st shot BFS, mm	2nd shot BFS, mm	3rd shot BFS, mm	4th shot BFS, mm	5th shot BFS, mm	6th shot BFS, mm	The layer where bullet stops	Specimen thickness, mm	Specimen weight, kg	Average projectile speed, m/s
Dry Kevlar	36,77	36,38	33,74	35,71	41,76	35,02	15	5,75	0,65	387,5
30% STF/Kevlar	38,58	29,48	44,09	31,17	Penetrated	Penetrated	-	6,6	1,20	392,8
40% STF/Kevlar	28,95	29,29	27,27	23,15	24,65	28,64	16	7,7	1,1	395,5
50% STF/Kevlar	27,66	35,19	29,70	32,49	28,4	32,95	17	9,3	1,05	394,5

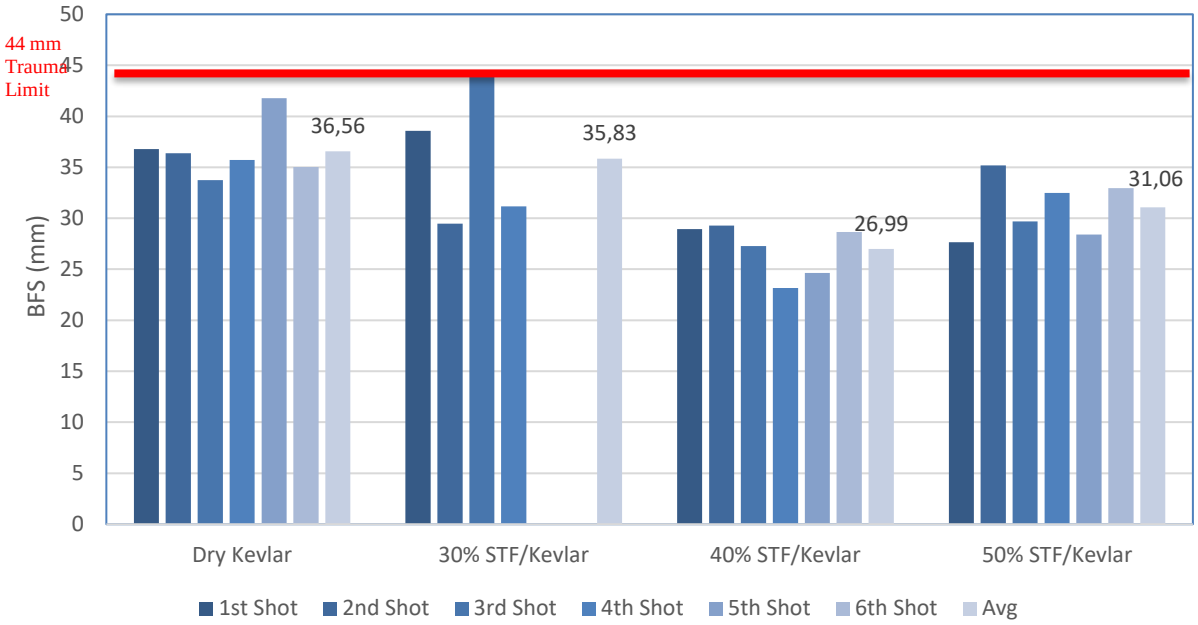

Fig. 9 BFS graph

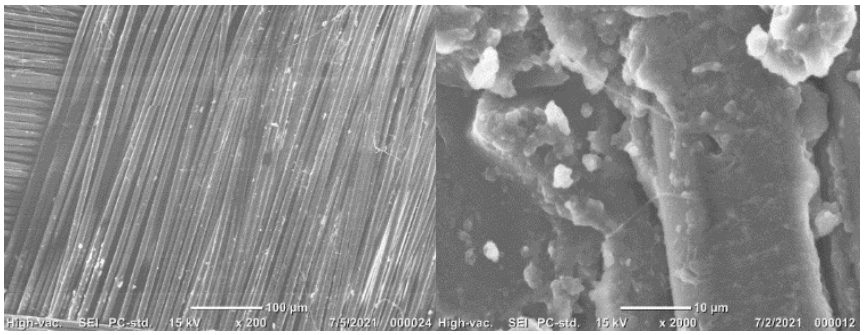

a b

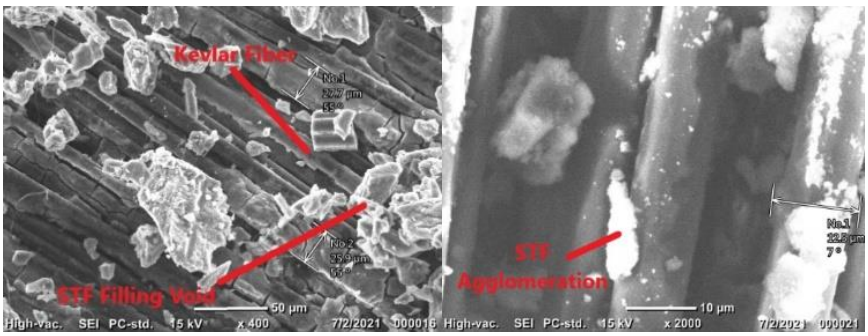

c d

Fig. 10 a) Untreated fabric; b) 30% STF/Kevlar; c) 40% STF/Kevlar; d) 50% STF/Kevlar

The reason why 50% STF/Kevlar performs less than 40% sample; it is considered as the increase in clumping in the liquid and the lack of polyethylene glycol, which is the holding media that will fill the yarns sufficiently as

in other samples. Although it is thought that ballistic behavior is improved with the increase in friction between the yarns in 50% STF/Kevlar structure, it is understood that shear thickening remains relatively weak compared to the others. It is believed that 50% silica STF reached saturation. In addition, it is expected that the trauma values will be much lower if the middle section of the fabrics stitched along with the edges. Due to the difficulty of such sewing operations, it is necessary to turn to alternative production methods in which the fabrics stick tightly together.

3.2.3. STF/Fabric SEM images

SEM images of fabrics are shown in Fig. 10. Images are taken with JEOL JCM 6000 PLUS. As can be seen in 30% and 40% STF/Kevlar samples, STF has largely covered the fibers, STF/Fiber integrity was also achieved by filling between the threads and forming a solid structure. However, the SEM image of 50% STF/Kevlar sample could not fill the gaps and cover the fibers like in other samples. SEM images and obtained ballistic and low speed impact tests are consistent with each other.

4. Conclusions

In this study, silica and polyethylene glycol used to create STF with different mass fractions, to understand the change of the ballistic performance of the fabrics with STF. Dry and liquid impregnated samples were subjected to low and high-speed impact tests.

Rheological measurements of the STF conducted using SEM. By investigating different silica concentrations in STF, it is understood that increasing silica nanoparticles in STF until 40 wt% is a substantial mechanism for the thickening behaviour. Because of the further increment of silica in STF, rheologic behaviour of 50% STF could not be observed. This is attributed to the non-uniform dispersion and lack of polyethylene glycol in STF.

Drop tower tests have shown that STF impregnation of fabrics increases impact resistance at low speeds. A witness sample was placed behind the aramid fabrics to prevent slipping, and the damage to the witness sample was examined along with the fabrics. It was observed that the damping increased as the silica content in the liquid increased. In addition, the findings were reflected in the damage seen by the witness plate.To understand the change in the behaviour of Kevlar fabrics, they were subjected to impacts at high speeds. After the liquid is prepared, the fabrics are immersed in the liquid, fed with a brush to ensure a uniform structure of the order possible and passed through double rollers. In high-speed tests, shots were fired in accordance with the NIJ 0101.06 standard. 9 mm ammunition was fired at a speed of 398±9 m/s at the NIJ II level at STF/Kevlar samples. 40% STF/Kevlar specimen showed the best ballistic performance among others. 40% STF/Kevlar fabric gave an average of 27% improved trauma results compared to dry Kevlar sample. While an improvement in ballistic behaviour is expected with an increase in the silica ratio, the performance of the 50% STF/Kevlar sample was weaker than the 40% STF/Kevlar sample, which is thought to be due to the lack of polyethylene glycol, that the liquid cannot enter sufficiently between the threads.

SEM images of dry and impregnated fabrics have been studied. Apart from the 50% STF/Kevlar sample, the other two liquid/fiber samples distributed better between the fabrics and formed a homogeneous structure by wrapping the fibers. The SEM images support the results obtained in the shot test. Low speed test results do agree well with the ballistic tests. It is believed that the shear-thickening materials may exhibit strong impact resistance for other fabrics, and they are expected to have potential in the soft body armor.

Acknowledgment

The authors acknowledge the support from CES Advanced Composite for providing Kevlar fabrics. Murat Berkay Zeka is grateful to the Pınar Acar Bozkurt of Ankara University providing support for this research.

References

1. **Wagner, N. J.; Brady, J. F.** 2009. Shear thickening in colloidal dispersions, Physics Today, p. 27-32. https://doi.org/10.1063/1.3248476.
2. **Lim, A. S.; Lopatnikov, S. L.; Wagner, N. J.; Gillespie, Jr. J. W**. 2010. Investigating the transient response of a shear thickening fluid using the split Hopkinson pressure bar technique, Rheol Acta 49: 879–890. https://doi.org/10.1007/s00397-010-0463-8.
3. **Boersma, W. H.; Laven, J.; Stein, H. N.** 1992. Viscoelastic properties of concentrated shear-thickening dispersions, Journal of Colloid and Interface Science 149(1): 10–22. https://doi.org/10.1016/0021-9797(92)90385-Y.
4. **Catherall, A. A.; Melrose, J. R.; Ball, R. C.** 2000. Shear thickening and order–disorder effects in concentrated colloids at high shear rates, Journal of Rheology 44(1): 1–25. https://doi.org/10.1122/1.551072.
5. **Brown, E.; Jaeger, H.M**. 2014. Shear thickening in concentrated suspensions: phenomenology, mechanisms and relations to jamming, Rep. Prog. Phys. 77: 1–23. https://doi.org/10.1088/0034-4885/77/4/046602.
6. **Hoffman, R. L.** 2020. Application of shear thickening fluids in material development, Journal of Materials Research and Technology 9(50): 10411-10433, https://doi.org/10.1016/j.jmrt.2020.07.049.
7. **Laun, H. M.; Bung, R.; Schmidt, F.** 1991. Rheology of extremely shear thickening polymer dispersions (passively viscosity switching fluids), Journal of Rheology 35: 999. https://doi.org/10.1122/1.550257.
8. **Gürgen, S.; Sofuoğlu, M. A.** 2020. Vibration attenuation of sandwich structures filled with shear thickening fluids, Composites Part B: Engineering 186: 107831. https://doi.org/10.1016/j.compositesb.2020.107831.
9. **Neagu, R. C.; Bourban, P. E.; Månson, J. E.** 2009. Micromechanics and damping properties of composites integrating shear thickening fluids, Composites Science and Technology 69(3-4): 515-22. https://doi.org/10.1016/j.compscitech.2008.11.019.
10. **Chen, K.; Wang, Y.; Xuan, S.; Gong, X.** 2017. A hybrid molecular dynamics study on the non-

Newtonian rheological behaviors of shear thickening fluid, Journal of Colloid and Interface Science 497: 378–384.
https://doi.org/10.1016/j.jcis.2017.03.038.
11. **Prabhu, T. A.; Singh, A.** 2021. Effect of carrier fluid and particle size distribution on the rheology of shear thickening suspensions, Rheol. Acta 60: 107–118.
https://doi.org/10.1007/s00397-021-01257-5.
12. **Saraç, M. F.; Peker, S.; Yapıcı, K.** 2018. Parçacık Boyutuna Bağlı Füme Silika Bazlı Kesme İle Kalınlaşan Akışkanların Reolojik Davranışı, Mühendislik Bilimleri ve Tasarım Dergisi 6(4): 665–671.
https://doi.org/10.21923/jesd.447357.
13. **Warren, J.; Offenberger, S.; Toghiani, H.; Pittman, Jr. C. U.; Lacy, T. E.; Kundu, S.** (2015. Effect of temperature on the shear-thickening behavior of fumed silica suspensions, ACS Applied Materials & Interfaces 7 (33): 18650-18661.
https://doi.org/10.1021/acsami.5b05094.
14. **Hoyle, C.; Dai, S.; Tanner, R.; Jabbarzadeh, A.** 2020. Effect of particle roughness on the rheology of suspensions of hollow glass microsphere particles, Journal of Non-Newtonian Fluid Mechanics 276: 104235.
https://doi.org/10.1016/j.jnnfm.2020.104235.
15. **Ancey, C.; Jorrot, H.** 2001. Yield stress for particle suspensions within a clay dispersion, Journal of Rheology 45(2): 297–319.
https://doi.org/10.1122/1.1343879.
16. **Lee, Y. S.; Wetzel, E. D.; Wagner, N. J.** 2003. The ballistic impact characteristics of Kevlar® woven fabrics impregnated with a colloidal shear thickening fluid, Journal of Materials Science 38(13): 2825–2833.
https://doi.org/10.1023/A:1024424200221.
17. **Bohannan, A.; Fahrenthold, E.** 2009. Simulation of STF Kevlar shielding performance in a stuffed whipple configuration, 50th AIAA/ASME/ASCE/AHS/ASC Structures, Structural Dynamics, and Materials Conference, Palm Springs, California.
https://doi.org/10.2514/6.2009-2400.
18. **Khodadadi, A.; Liaghat, G.; Bahramian, A. R.; Ahmadi, H.; Anani, Y.; Asemani, S.; Razmkhah, O.** 2019. High velocity impact behavior of Kevlar/rubber and Kevlar/epoxy composites: a comparative study, Composite Structures 216: 159–167.
https://doi.org/10.1016/j.compstruct.2019.02.080.
19. **Mawkhlieng, U.; Majumdar, A.** 2019). Deconstructing the role of shear thickening fluid in enhancing the impact resistance of high-performance fabrics, Composites Part B: Engineering 175: 107167.
https://doi.org/10.1016/j.compositesb.2019.107167.
20. **Li, W.; Xiong, D.; Zhao, X.; Sun, L.; Liu, J.** 2016. Dynamic stab resistance of ultra-high molecular weight polyethylene fabric impregnated with shear thickening fluid, Materials & Design 102: 162–167.
https://doi.org/10.1016/j.matdes.2016.04.006.
21. **Majumdar, A.; Butola, B. S.; Srivastava, A.** 2013. An analysis of deformation and energy absorption modes of shear thickening fluid treated Kevlar fabrics as soft body armour materials, Materials & Design 51: 148–153.
https://doi.org/10.1016/j.matdes.2013.04.016.
22. **Liu, L.; Cai, M.; Liu, X.; Zhao, Z.; Chen, W.** 2020. Ballistic impact performance of multi-phase STF-impregnated Kevlar fabrics in aero-engine containment, Thin-Walled Structures 157: 107103.
https://doi.org/10.1016/j.tws.2020.107103.
23. **Gürgen, S.; Kuşhan, M. C.** 2017. The stab resistance of fabrics impregnated with shear thickening fluids including various particle size of additives, Composites Part A: Applied Science and Manufacturing 94: 50–60.
https://doi.org/10.1016/j.compositesa.2016.12.019.
24. NIJ Guide. Guide of Body Armor Selection, Application Guide 0101.06 to Ballistic-Resistant Body Armor. 2014, Washington: U.S. National Instute of Justice.

M. B. Zeka, A. Aytaç

INVESTIGATION OF IMPACT PERFORMANCE OF STF IMPRAGNATED COMPOSITES

S u m m a r y

It is important to achieve high strength, high modulus of elasticity, good energy damping for lightweight armor materials. For this purpose, two or more similar or different materials are combined at the macro level. In this way, a new structure emerges that we call composite material. A composite is a new structure in which the good properties of the components in its structure become evident in the material. Research on the production and mechanical properties of composites that meet the needs of the developing technology continues. Military personnel, armored vehicles and many security elements are tested in the field with a lot of threats (such as mines, armor piercing ammunition, explosives etc.). Therefore, the armor used by security elements should be strengthened without compromising features such as lightness, cost and long-term use. This study covers the development of Kevlar's ballistic properties by impregnating Shear Thickening Fluid (STF). STF is composed of silica (AEROSIL 200) and polyethylene glycol (PEG 400). STF-impregnated Kevlar fibers have been subjected to impact testing at low and high speeds. Low-speed tests were carried out with a drop tower. High-speed tests were carried out according to NIJ 0101.06 Level II standards. The mass fraction of silica in the STF was determined as the research parameter. The change in the behavior of the materials with the change of silica ratio was investigated; Although improvements were observed in energy dissipation in low-speed impacts, it was noted that ballistic behavior improved up to a certain point, and then the improvement in behavior decreased.

Keywords: shear thickening fluid, kevlar, drop test, ballistic performance, aramid.

Received April 3, 2022
Accepted April 5, 2023